Physics Letters B 843 (2023) 138009

Contents lists available at ScienceDirect

Physics Letters B

journal homepage: www.elsevier.com/locate/physletb

Consistency of new CDF-II W boson mass with 123-model

B. Ait Ouazghour [a], R. Benbrik [b], E. Ghourmin [c], M. Ouchemhou [b], L. Rahili [c,*]

[a] LPHEA, Faculty of Science Semlalia, Cadi Ayyad University, P.O.B. 2390 Marrakech, Morocco
[b] Polydisciplinary Faculty, Laboratory of Fundamental and Applied Physics, Cadi Ayyad University, Sidi Bouzid, B.P. 4162, Safi, Morocco
[c] Laboratory of Theoretical and High Energy Physics, Faculty of Science, Ibnou Zohr University, B.P 8106, Agadir, Morocco

ARTICLE INFO

Article history:
Received 7 February 2023
Received in revised form 3 June 2023
Accepted 6 June 2023
Available online 12 June 2023
Editor: J. Hisano

ABSTRACT

Following the recent update measurement of the W boson mass performed by the CDF-II experiment at Fermilab which indicates 7σ deviation from the SM prediction. As a consequence, the open question is whether there are extensions of the SM that can carry such a remarkable deviation or what phenomenological repercussions this has. In this paper, we investigate what the theoretical constraints reveal about the 123-model. Also, we study the consistency of a CDF W boson mass measurement with the 123-model expectations, taking into account theoretical and experimental constraints. Both fit results of S and T parameters before and after $m_W^{\rm CDF}$ measurement are, moreover, considered in this study. Under these conditions, we found that the 123-model prediction is consistent with the measured $m_W^{\rm CDF}$ at a 95% Confidence Level (CL).

1. Introduction

High-precision measurements at collider experiments have enacted strict constraints on the Standard Model (SM) and its possible extensions. The experimental accuracy of the electroweak observables is sensitive to the radiative corrections and needs the highest precision on the theoretical side as well. This precision measurement has been remarkably corroborated by the discovery of a Higgs particle at the LHC experiment [1,2]. Moreover, it provides a pathway for deriving indirect hints on heavy new physics BSM, in particular on the not yet sufficiently explored scalar sector. In this regard, any extension of the SM is required to fulfill the $\rho \approx 1$ constraint (it is explained as being the ratio of neutral to charged current at low momentum.), which is favored by experimental data allowing just a little departure from unity. Such a deviation, $\Delta\rho$, comes from the radiative correction taking place in the models with an extra Higgs field. $\Delta\rho$ can be related to the vector-boson self-energies and have the biggest impact in the higher-order computation of precision observables, which is a major factor to accurately measured quantities such as m_W, m_Z as well as the effective weak mixing angle $\sin^2\theta_{\rm eff}$.

Recently, the CDF collaboration has released their newly measured W boson mass [3]:

$$m_W^{\rm CDF} = 80.4335 \pm 0.0094\ {\rm GeV}, \tag{1}$$

which is out of the range of the SM prediction of about 7σ, which is given by [4,5] as follows:

$$m_W^{\rm SM} = 80.357 \pm 0.006\ {\rm GeV}. \tag{2}$$

Such a large deviation strongly indicates the existence of an emerging field of novel physics related to Spontaneous Symmetry Breaking (SSB), such as models with extended Higgs sectors.

In this paper, we focus on the 123-model to investigate the possibility of predicting m_W according to the new CDF measurement. The model can provide a stable candidate for dark matter and explain the tiny neutrino mass. Its scalar sector contains three CP-even Higgs bosons, h_1, h_2 and h_3, one CP-odd Higgs boson, A, a pair of charged Higgs bosons, $H^{\pm}$, and a pair of double-charged Higgs bosons, $H^{\pm\pm}$. Recently, several novel physics models, including the: two-Higgs doublet model [6–20], Higgs Triplet Model (HTM) [21–25],

* Corresponding author.
E-mail addresses: brahim.aitouazghour@edu.uca.ac.ma (B. Ait Ouazghour), r.benbrik@uca.ma (R. Benbrik), s.ghourmin123@gmail.com (E. Ghourmin), mohamed.ouchemhou@ced.uca.ac.ma (M. Ouchemhou), rahililarbi@gmail.com (L. Rahili).

https://doi.org/10.1016/j.physletb.2023.138009

Supersymmetry [26–30], Leptoquark Model [31–33], Seesaw mechanism [34–38], Vector-Like Leptons and/or Vector-Like Quarks [39–44] and other SM extensions [45–58] are proposed to explain the W boson mass anomaly.

The correction of the 123-model to W boson mass can be parameterized by the S, T, and U formalism as follows: [59]:

$$\Delta m_W^2 = \left(m_W^{123}\right)^2 - \left(m_W^{\rm SM}\right)^2 = \frac{\alpha_0 c_W^2 m_Z^2}{c_W^2 - s_W^2}\left[-\frac{1}{2}S + c_W^2 T + \frac{c_w^2 - s_w^2}{4 s_W^2}U\right], \tag{3}$$

where α_0 is the fine structure constant at the Thomson limit, θ_w is the Weinberg angle, m_Z is the Z gauge boson mass, and $s_x\,(c_x)$ stands for $\sin x$ ($\cos x$).

The same formalism can, moreover, be used to study the effective weak mixing angle, $\sin^2\theta_{\rm eff}$, using the following relation:

$$\Delta \sin^2\theta_{\rm eff} = \sin^2\theta_{\rm eff}\Big|_{123} - \sin^2\theta\Big|_{\rm SM} = \frac{\alpha_0}{c_W^2 - s_W^2}\left[\frac{1}{4}S - s_W^2 c_W^2 T\right], \tag{4}$$

wherein the SM values used are listed in Ref. [4]. The rest of the paper is organized as follows. In Sec. 2, we describe in great length the 123-model, and then explain the theoretical investigations applied to its parameter space in Sec. 3. In Sec. 4, we highlight the new physics contribution to S and T oblique parameters. Based on these considerations, our main results are discussed in Sec. 5 and finally, we summarize our conclusions in Sec. 6.

2. The 123-model

Firstly adapted in [60], the 123-model has been the focus of many studies in the past dozen years [61], the results of which provide considerable information and open up a window for new physics beyond the standard model. Nevertheless, the importance of theoretical discussions cannot be underestimated. This section sets out a brief overview of the general 123-model, including the involved multiplets, minimization conditions, and a whole discussion on Higgs bosons, gauge bosons, and neutrino mass generation in the framework of 123-mechanism.

2.1. The scalar potential

In addition to the usual SM scalar doublet, namely ϕ, a singlet σ, and a triplet Δ have been added together to fundamentally build blocks for the 123-model. Bearing in mind its representations under the $SU(3)_c \times SU(2)_L \times U(1)_Y$ SM gauge group, one could explicitly write

$$\begin{aligned}
\sigma(1,1,+0) &= \frac{1}{\sqrt{2}}(v_\sigma + R_\sigma + iI_\sigma),\\
\phi(1,2,+\frac{1}{2}) &= \begin{pmatrix} \frac{1}{\sqrt{2}}(v_\phi + R_\phi + iI_\phi) \\ \phi^- \end{pmatrix},\\
\Delta(1,3,+1) &= \begin{pmatrix} \frac{1}{\sqrt{2}}(v_\Delta + R_\Delta + iI_\Delta) & \Delta^+/\sqrt{2} \\ \Delta^+/\sqrt{2} & \Delta^{++} \end{pmatrix},
\end{aligned} \tag{5}$$

with corresponding leptonic numbers $L_\sigma = 2$, $L_\phi = 0$ and $L_\Delta = -2$, respectively.

The most general renormalizable and gauge-invariant Lagrangian of the 123-scalar sector is given by

$$\mathcal{L} = (D_\mu\phi)^\dagger(D^\mu\phi) + Tr(D_\mu\Delta)^\dagger(D^\mu\Delta) + (\partial_\mu\sigma)^\dagger(\partial^\mu\sigma) - V(H,\Delta) + \mathcal{L}_{\rm Yukawa}, \tag{6}$$

with the covariant derivatives in the kinetic terms are

$$\begin{aligned}
D_\mu\phi &= \partial_\mu\phi + igT^a W_\mu^a\phi + i\frac{1}{2}g' B_\mu\phi,\\
D_\mu\Delta &= \partial_\mu\Delta + ig[T^a W_\mu^a, \Delta] + ig'\frac{Y_\Delta}{2}B_\mu\Delta,
\end{aligned} \tag{7}$$

where W_μ^a and B_μ stand for $SU(2)_L$ and $U(1)_Y$ gauge fields, respectively. Y_Δ is the hypercharge operator of the triplet Δ, while T^a is related to the Pauli matrices via $T^a = \sigma^a/2$. $\mathcal{L}_{\rm Yukawa}$ refer to the Yukawa part to be subsequently considered in detail.

The scalar potential $V(\sigma,\phi,\Delta)$, invariant under $SU(2)_L \times U(1)_Y$, reads [62,63]

$$\begin{aligned}
V(\sigma,\phi,\Delta) = {}& \mu_\sigma^2\sigma^\dagger\sigma + \mu_\phi^2\phi^\dagger\phi + \mu_\Delta^2 {\rm Tr}(\Delta^\dagger\Delta) + \lambda_1(\phi^\dagger\phi)^2 + \lambda_2\left[{\rm Tr}(\Delta^\dagger\Delta)\right]^2 + \lambda_3(\phi^\dagger\phi){\rm Tr}(\Delta^\dagger\Delta)\\
&+ \lambda_4{\rm Tr}(\Delta^\dagger\Delta\Delta^\dagger\Delta) + \lambda_5(\phi^\dagger\Delta^\dagger\Delta\phi) + \beta_1(\sigma^\dagger\sigma)^2 + \beta_2(\phi^\dagger\phi)(\sigma^\dagger\sigma) + \beta_3{\rm Tr}(\Delta^\dagger\Delta)(\sigma^\dagger\sigma) - \kappa(\phi^T\Delta\phi\sigma + {\rm h.c.}),
\end{aligned} \tag{8}$$

where all quartic couplings are considered to be real. μ_i^2 $(i = \sigma,\phi,\Delta)$ are squared mass parameters of the singlet, doublet, and triplet fields, respectively. These parameters can be eliminated by imposing the following vacuum conditions:

$$\begin{aligned}
2v_\sigma\mu_\sigma^2 &= \kappa v_\Delta v_\phi^2 - 2\beta_1 v_\sigma^3 - \beta_2 v_\sigma v_\phi^2 - \beta_3 v_\sigma v_\Delta^2,\\
2\mu_\phi^2 &= 2\kappa v_\sigma v_\Delta - \beta_2 v_\sigma^2 - 2\lambda_1 v_\phi^2 - \lambda_3 v_\Delta^2 - \lambda_5 v_\Delta^2,\\
2v_\Delta\mu_\Delta^2 &= \kappa v_\sigma v_\phi^2 - \beta_3 v_\sigma^2 v_\Delta - 2\lambda_2 v_\Delta^3 - \lambda_3 v_\Delta v_\phi^2 - 2\lambda_4 v_\Delta^3 - \lambda_5 v_\Delta v_\phi^2,
\end{aligned} \tag{9}$$

thereby reducing the set of free parameters down by three degree-of-freedom.

2.2. The field composition of the model

The next stage is to extract from the Lagrangian basis the usual mass matrices for the 123-model. The bilinear part of the Higgs potential in Eq. (8) is given by

$$V(\sigma,\phi,\Delta) \supset \left(\delta^{--}\right)\mathcal{M}^2_{\delta^{\pm\pm}}\left(\delta^{++}\right) + \left(\phi^-,\delta^-\right)\mathcal{M}^2_{\phi^\pm\delta^\pm}\begin{pmatrix}\phi^+\\ \delta^+\end{pmatrix} + \frac{1}{2}\left(R_\sigma,R_\phi,R_\Delta\right)\mathcal{M}^2_R\begin{pmatrix}R_\sigma\\ R_\phi\\ R_\Delta\end{pmatrix} + \frac{1}{2}\left(I_\sigma,I_\phi,I_\Delta\right)\mathcal{M}^2_I\begin{pmatrix}I_\sigma\\ I_\phi\\ I_\Delta\end{pmatrix} + \cdots \tag{10}$$

where $\mathcal{M}^2_{\delta^{\pm\pm}}$, $\mathcal{M}^2_{\phi^\pm\delta^\pm}$, $\mathcal{M}^2_R$ and $\mathcal{M}^2_I$ are 1×1, 2×2, 3×3 and 3×3 mass matrices of the doubly charged, simply charged, CP-even sector and CP-odd sector, respectively.

At tree-level and without any assumption except Eq. (9), the three entries of the scalar and pseudo-scalar Higgs sector matrices are given by [63]

$$\begin{aligned}
&(\mathcal{M}_R)^2_{11} = 2\beta_1 v_\sigma^2 + \frac{1}{2}\kappa v_\phi^2\frac{v_\Delta}{v_\sigma}, && (\mathcal{M}_I)^2_{11} = \frac{1}{2}\kappa v_\phi^2\frac{v_\Delta}{v_\sigma},\\
&(\mathcal{M}_R)^2_{22} = 2\lambda_1 v_\phi^2, && (\mathcal{M}_I)^2_{22} = 2\kappa v_\Delta v_\sigma,\\
&(\mathcal{M}_R)^2_{33} = 2(\lambda_2+\lambda_4)v_\Delta^2 + \frac{1}{2}\kappa v_\phi^2\frac{v_\sigma}{v_\Delta}, && (\mathcal{M}_I)^2_{33} = \frac{1}{2}\kappa v_\phi^2\frac{v_\sigma}{v_\Delta},\\
&(\mathcal{M}_R)^2_{12} = \beta_2 v_\phi v_\sigma - \kappa v_\phi v_\Delta = (\mathcal{M}_R)^2_{21}, && (\mathcal{M}_I)^2_{12} = \kappa v_\phi v_\Delta = (\mathcal{M}_I)^2_{21},\\
&(\mathcal{M}_R)^2_{13} = \beta_3 v_\Delta v_\sigma - \frac{1}{2}\kappa v_\phi^2 = (\mathcal{M}_R)^2_{31}, && (\mathcal{M}_I)^2_{13} = \frac{1}{2}\kappa v_\phi^2 = (\mathcal{M}_I)^2_{31},\\
&(\mathcal{M}_R)^2_{23} = (\lambda_3+\lambda_5)v_\phi v_\Delta - \kappa v_\phi v_\sigma = (\mathcal{M}_R)^2_{32}, && (\mathcal{M}_I)^2_{23} = \kappa v_\phi v_\sigma = (\mathcal{M}_I)^2_{32},
\end{aligned} \tag{11}$$

while for the charged sectors read as [63],

$$\begin{aligned}
&\left(\mathcal{M}^2_{\delta^{\pm\pm}}\right) = -\lambda_4 v_\Delta^2 - \frac{1}{2}\lambda_5 v_\phi^2 + \frac{1}{2}\kappa v_\phi^2\frac{v_\sigma}{v_\Delta},\\
&\left(\mathcal{M}_{\phi^\pm\delta^\pm}\right)^2_{11} = -\frac{1}{2}\lambda_5 v_\Delta^2 + \kappa v_\Delta v_\sigma,\\
&\left(\mathcal{M}_{\phi^\pm\delta^\pm}\right)^2_{22} = -\frac{1}{4}\lambda_5 v_\phi^2 + \frac{1}{2}\kappa v_\phi^2 v_\sigma/v_\Delta,\\
&\left(\mathcal{M}_{\phi^\pm\delta^\pm}\right)^2_{12} = \frac{1}{2\sqrt{2}}\lambda_5 v_\Delta v_\phi - \frac{1}{\sqrt{2}}\kappa v_\phi v_\sigma = \left(\mathcal{M}_{\phi^\pm\delta^\pm}\right)^2_{21}.
\end{aligned} \tag{12}$$

By applying a unitary transformation in the non-physical fields basis, one can get the mass eigenstates in the lowest order as follows:

$$\begin{pmatrix}h_1\\ h_2\\ h_3\end{pmatrix} = U^H\cdot\begin{pmatrix}R_\sigma\\ R_\phi\\ R_\Delta\end{pmatrix}, \quad \begin{pmatrix}G\\ J\\ A\end{pmatrix} = U^A\cdot\begin{pmatrix}I_\sigma\\ I_\phi\\ I_\Delta\end{pmatrix} \quad \text{and} \quad \begin{pmatrix}G^\pm\\ H^\pm\end{pmatrix} = U^C\cdot\begin{pmatrix}\phi^\pm\\ \Delta^\pm\end{pmatrix}. \tag{13}$$

The two 3×3 matrices U^H and U^A transform the neutral CP-even and CP-odd Higgs fields, respectively. They take the following form [63,64]:

$$U^H = \begin{pmatrix} c_{\alpha_1}c_{\alpha_2} & s_{\alpha_1}c_{\alpha_2} & s_{\alpha_2}\\ -(c_{\alpha_1}s_{\alpha_2}s_{\alpha_3}+s_{\alpha_1}c_{\alpha_3}) & c_{\alpha_1}c_{\alpha_3}-s_{\alpha_1}s_{\alpha_2}s_{\alpha_3} & c_{\alpha_2}s_{\alpha_3}\\ -c_{\alpha_1}s_{\alpha_2}c_{\alpha_3}+s_{\alpha_1}s_{\alpha_3} & -(c_{\alpha_1}s_{\alpha_3}+s_{\alpha_1}s_{\alpha_2}c_{\alpha_3}) & c_{\alpha_2}c_{\alpha_3}\end{pmatrix} = V_{\text{PMNS}}, \tag{14}$$

$$U^A = \begin{pmatrix} 0 & \frac{1}{N_G} & -\frac{2}{N_G}\frac{v_\Delta}{v_\phi}\\ \frac{N_G^2}{N_J} & -\frac{2}{N_J}\frac{v_\Delta^2}{v_\phi v_\sigma} & -\frac{1}{N_J}\frac{v_\Delta}{v_\sigma}\\ \frac{1}{N_A}\frac{v_\Delta}{v_\sigma} & \frac{2}{N_A}\frac{v_\Delta}{v_\phi} & \frac{1}{N_A}\end{pmatrix}. \tag{15}$$

The mixing angles $\alpha_{1,2,3}$ could lie within the range $[-\pi/2,+\pi/2]$, and $N_{G,J,A}$ are defined as follows

$$N_G = \sqrt{1+4\frac{v_\Delta^2}{v_\phi^2}},\ N_J = \sqrt{N_G^4+4\frac{v_\Delta^4}{v_\phi^2 v_\sigma^2}+\frac{v_\Delta^2}{v_\sigma^2}} \text{ and } N_A = \sqrt{1+4\frac{v_\Delta^2}{v_\phi^2}+\frac{v_\Delta^2}{v_\sigma^2}}, \tag{16}$$

whereas U^C is the matrix that transforms the charged Higgs field which is given by its 2×2 representation $\{\{-c_\beta,s_\beta\},\{s_\beta,c_\beta\}\}$. s_β (c_β) stands for $\sin\beta$ $(\cos\beta)$ satisfying $t_\beta=\tan\beta=\sqrt{2}v_\Delta/v_\phi$.

Based on the foregoing, the Higgs sector of 123-model is made up of nine scalar bosons, five of them being electrically neutral (denoted usually as h_1, h_2, h_3, A and the Majoron J) and the other four charged ($H^{\pm}$ and $H^{\pm\pm}$). Their masses can be written as

$$\text{diag}(m^2_{h_1}, m^2_{h_2}, m^2_{h_3}) = U^H \mathcal{M}_R U^{H^{\mathrm{T}}}, \tag{17}$$

$$m^2_A = \frac{1}{2}\kappa\left(\frac{v_\sigma v^2_\phi}{v_\Delta} + \frac{v_\Delta v^2_\phi}{v_\sigma} + 4 v_\sigma v_\Delta\right), \tag{18}$$

$$m^2_J = 0, \tag{19}$$

$$m^2_{H^\pm} = \frac{1}{2}\left(\kappa\frac{v_\sigma}{v_\Delta} - \frac{1}{2}\lambda_5\right)\left(v^2_\phi + 2v^2_\Delta\right), \tag{20}$$

$$m^2_{H^{\pm\pm}} = -\lambda_4 v^2_\Delta - \frac{1}{2}\lambda_5 v^2_\phi + \frac{1}{2}\kappa v^2_\phi \frac{v_\sigma}{v_\Delta}. \tag{21}$$

Here the Majoron J is the second massless physical Higgs in the CP-odd sector to be predominantly singlet, matching the consistency of the 123-model with the LEP measurements of the invisible Z decay width [65,66]. Furthermore, it is worth to mention that a different hierarchy between $H^{\pm\pm}$, $H^{\pm}$ and A masses can occur, and mainly depends on λ_5 sign, resulting in splitting that is described by (assuming $v_\Delta \ll v_\phi$)

$$\Delta m^2 \approx m^2_{H^{\pm\pm}} - m^2_{H^\pm} \approx m^2_{H^\pm} - m^2_A \approx \frac{1}{2}(m^2_{H^{\pm\pm}} - m^2_A). \tag{22}$$

2.3. The model parameters

Let's begin by setting two redefinitions of VEV's as follows:

$$v^2 = v^2_\phi + 2v^2_\Delta \quad \text{and} \quad v^4_0 = 4v^2_\sigma v^2_\Delta + v^2_\phi(v^2_\sigma + v^2_\Delta), \tag{23}$$

in terms of the physical basis parameters, the dimensionless quartic couplings, λ_i, of the 123-potential, which read

$$\kappa = \frac{2v_\sigma v_\Delta}{v^4_0} m^2_A \tag{24}$$

$$\lambda_1 = \frac{1}{2v^2_\phi}\sum_{i=1}^{3}(U^H_{i2})^2 m^2_{h_i} \tag{25}$$

$$\lambda_2 = \frac{1}{2v^2_\Delta}\left(\sum_{i=1}^{3}(U^H_{i3})^2 m^2_{h_i} - 4\frac{v^2_\phi}{v^2}m^2_{H^\pm} + 2m^2_{H^{\pm\pm}} + \frac{v^2_\phi v^2_\sigma}{v^4_0}m^2_A\right) \tag{26}$$

$$\lambda_3 = \frac{1}{v_\phi v_\Delta}\sum_{i=1}^{3} U^H_{i2}U^H_{i3} m^2_{h_i} + \frac{4}{v^2}m^2_{H^\pm} - \frac{2v^2_\sigma}{v^4_0}m^2_A \tag{27}$$

$$\lambda_4 = \frac{1}{v^2_\Delta}\left(2\frac{v^2_\phi}{v^2}m^2_{H^\pm} - m^2_{H^{\pm\pm}} - \frac{v^2_\sigma v^2_\phi}{v^4_0}m^2_A\right) \tag{28}$$

$$\lambda_5 = 4\left(\frac{v^2_\sigma}{v^4_0}m^2_A - \frac{1}{v^2}m^2_{H^\pm}\right) \tag{29}$$

$$\beta_1 = \frac{1}{2v^2_\sigma}\left(\sum_{i=1}^{3}(U^H_{i1})^2 m^2_{h_i} - \frac{v^2_\phi v^2_\Delta}{v^4_0}m^2_A\right) \tag{30}$$

$$\beta_2 = \frac{1}{v_\sigma v_\phi}\left(\sum_{i=1}^{3} U^H_{i1}U^H_{i2} m^2_{h_i} + \frac{2v_\sigma v_\phi v^2_\Delta}{v^4_0}m^2_A\right) \tag{31}$$

$$\beta_3 = \frac{1}{v_\sigma v_\Delta}\left(\sum_{i=1}^{3} U^H_{i1}U^H_{i3} m^2_{h_i} + \frac{v_\sigma v^2_\phi v_\Delta}{v^4_0}m^2_A\right) \tag{32}$$

To end with this part, the 123-model, in total, is described by 12 independent real degrees of freedom. By considering the further constraint $v = \sqrt{v^2_\phi + 4v^2_\Delta}$ arising from the correct electroweak scale requirements, and using the previous Eq. (9) to trade the three multiplet masses for the SM Vacuum Expectation Value (VEV) v, t_β and v_S. Thus, we use the following hybrid set of input parameters:

$$m_{h_1}\,,\ m_A\,,\ \lambda_j\,(i=2,4,5)\,,\ m_{H^\pm}\,,\ \beta_3\,,\ \alpha_{i\,(i=1,2,3)}\,,\ v_\sigma\,,\ v_\Delta. \tag{33}$$

Table 1
Basis states and eigenvalues of the complete set of 2-body scalar scattering processes matrix $\mathcal{M}$, categorized based on the overall charge Q of the initial and final states.

Q	Basis states	Eigenvalues
0	$\mathcal{B}_1 = \{\phi^+\delta^-,\ \delta^+\phi^-,\ R_\phi I_\Delta,\ R_\phi I_\sigma,\ R_\Delta I_\phi,\ R_\Delta I_\sigma,\ R_\sigma I_\phi,\ R_\sigma I_\Delta,\ R_\sigma R_\Delta,\ R_\sigma R_\phi,\ R_\phi R_\Delta,\ I_\sigma I_\Delta,\ I_\sigma I_\phi,\ I_\phi I_\Delta\}$	$a_1^+,\ a_1^-,\ b_1,\ b_2,\ b_3$ b_4
0	$\mathcal{B}_2 = \{\phi^+\phi^-,\ \delta^+\delta^-,\ \delta^{++}\delta^{--},\ R_\phi R_\phi/\sqrt{2},\ R_\Delta R_\Delta/\sqrt{2},$ $R_\sigma R_\sigma/\sqrt{2},\ I_\phi I_\phi/\sqrt{2},\ I_\Delta I_\Delta/\sqrt{2},\ I_\sigma I_\sigma/\sqrt{2}\}$	$a_2^+,\ a_2^-,\ b_5,\ b_6,\ b_7$ $b_8,\ b_{9\ldots11}$
0	$\mathcal{B}_3 = \{R_\phi I_\phi,\ R_\Delta I_\Delta,\ R_\sigma I_\sigma\}$	$b_5,\ b_6,\ b_8$
1	$\mathcal{B}_4 = \{R_\phi\phi^+,\ R_\Delta\phi^+,\ R_\sigma\phi^+,\ I_\phi\phi^+,\ I_\Delta\phi^+,\ I_\sigma\phi^+,\ R_\phi\delta^+,$ $R_\Delta\delta^+,\ R_\sigma\delta^+,\ I_\phi\delta^+,\ I_\Delta\delta^+,\ I_\sigma\delta^+,\ \delta^{++}\phi^-,\ \delta^{++}\delta^-\}$	$a_1^+,\ a_1^-,\ a_2^+,\ a_2^-,\ a_3^+,\ a_3^-$ $b_1,\ b_2,\ b_3,\ b_4,\ b_7,\ b_8,\ b_{12}$
2	$\mathcal{B}_5 = \{\phi^+\phi^+/\sqrt{2},\ \delta^+\delta^+/\sqrt{2},\ \phi^+\delta^+,\ \delta^{++}R_\phi,\ \delta^{++}R_\Delta,$ $\delta^{++}R_\sigma,\ \delta^{++}I_\phi,\ \delta^{++}I_\Delta,\ \delta^{++}I_\sigma\}$	$a_3^+,\ a_3^-,\ b_2,\ b_3,\ b_4$ $b_7,\ b_8,\ b_{12},\ b_{13}$
3	$\mathcal{B}_6 = \{\delta^{++}\phi^+,\ \delta^{++}\delta^+\}$	$b_3,\ b_8$
4	$\mathcal{B}_7 = \{\delta^{++}\delta^{++}/\sqrt{2}\}$	b_8

3. Theoretical constraints on Lagrangian parameters

Before proceeding with a complete scan over the whole space parameters, it may be recalled that the 123-model has been and continues to be a matter of many theoretical and experimental investigations. The first one relates mainly to: boundedness from below of the scalar potential, perturbative unitarity, and the global minimum that the potential must preserve.

3.1. Vacuum stability

A prerequisite was to ensure that scalar potential of the 123-model is bounded from below, where the quartic terms assert itself at large field strength ($V > -\infty$). Following the same methodology as in [67–70], the authors in [71] have derived the constraints ensuring BFB and the corresponding whole set read:

$$
\begin{aligned}
\lambda_1 &> 0, & \beta_1 &> 0,\\
\lambda_2+\lambda_4 &> 0, & \beta_2+2\kappa+2\sqrt{\beta_1\lambda_1} &> 0,\\
\lambda_2+\lambda_4/2 &> 0, & \beta_2-2\kappa+2\sqrt{\beta_1\lambda_1} &> 0,\\
\lambda_3+2\kappa+2\sqrt{\lambda_1(\lambda_2+\lambda_4)} &> 0, & \beta_3+2\kappa+2\sqrt{\beta_1(\lambda_2+\lambda_4)} &> 0,\\
\lambda_3+2\kappa+2\sqrt{\lambda_1(\lambda_2+\lambda_4/2)} &> 0, & \beta_3+2\kappa+2\sqrt{\beta_1(\lambda_2+\lambda_4/2)} &> 0,\\
\lambda_3+\lambda_5+2\kappa+2\sqrt{\lambda_1(\lambda_2+\lambda_4/2)} &> 0, & \beta_3-2\kappa+2\sqrt{\beta_1(\lambda_2+\lambda_4/2)} &> 0,\\
\lambda_3+\lambda_5+2\kappa+2\sqrt{\lambda_1(\lambda_2+\lambda_4)} &> 0, & \beta_3-2\kappa+2\sqrt{\beta_1(\lambda_2+\lambda_4/2)} &> 0,\\
\lambda_3-2\kappa+2\sqrt{\lambda_1(\lambda_2+\lambda_4/2)} &> 0, & \beta_3-2\kappa+2\sqrt{\beta_1(\lambda_2+\lambda_4)} &> 0,\\
\lambda_3-2\kappa+2\sqrt{\lambda_1(\lambda_2+\lambda_4)} &> 0, & &\\
\lambda_3+\lambda_5-2\kappa+2\sqrt{\lambda_1(\lambda_2+\lambda_4/2)} &> 0, & &\\
\lambda_3+\lambda_5-2\kappa+2\sqrt{\lambda_1(\lambda_2+\lambda_4)} &> 0, & &
\end{aligned}
\tag{34}
$$

3.2. $\mathcal{S}-$matrix unitarity

A closer look reveals that the entire set of 2-body scalar scattering processes results in a 52×52 S-matrix that can be split up into 7 block submatrices representing mutually unmixed groups of channels with definite charge and CP states, organized in a database $\mathcal{B}_i$ in terms of net electric charge in the initial/final states: $\mathcal{B}_1(14\times14)$, $\mathcal{B}_2(9\times9)$ and $\mathcal{B}_3(3\times3)$, corresponding to 0-charge channels, $\mathcal{B}_4(14\times14)$ corresponding to the 1-charge channels, $\mathcal{B}_5(9\times9)$ corresponding to the 2-charge channels, $\mathcal{B}_6(2\times2)$ corresponding to the 3-charge channels, and finally $\mathcal{B}_7(1\times1)$ corresponding to the 4-charge channels. The following Table 1 highlights an illustration of the framework described above.

The complete set of eigenvalues electromagnetism, described as combinations of λ's couplings are given by:

$$
\begin{aligned}
b_1 &= \beta_2, & a_1^\pm &= \frac{1}{4}\Big(2\beta_2+2\lambda_3+3\lambda_5 \pm \sqrt{(2\beta_2-2\lambda_3-3\lambda_5)^2+96\kappa^2}\Big)\\
b_2 &= \lambda_3, & a_2^\pm &= \lambda_1+\lambda_2+2\lambda_4 \pm \sqrt{(\lambda_1-\lambda_2-2\lambda_4)^2+\lambda_5^2},\\
b_3 &= \lambda_3+\lambda_5, & a_3^\pm &= \frac{1}{2}\Big(\beta_3+2\lambda_1 \pm \sqrt{(\beta_3-2\lambda_1)^2+8\kappa^2}\Big),\\
b_4 &= \beta_3, & b_8 &= 2\Big(\lambda_2+\lambda_4\Big),\\
b_5 &= 2\beta_1, & b_{12} &= \lambda_3-\frac{1}{2}\lambda_5,
\end{aligned}
$$

$$b_6 = 2\lambda_1, \qquad b_{13} = 2\lambda_2 - \lambda_4,$$
$$b_7 = 2\lambda_2. \tag{35}$$

whereas the remaining $b_{9\ldots11}$ eigenvalues are the roots of a third-order equation given by

$$x^3 - 8\Big[3\lambda_1 + 3\lambda_4 + 4\lambda_2 + 2\beta_1\Big]x^2 + 8\Big[8\big(3\lambda_1(4\lambda_2 + 3\lambda_4) + \beta_1(6\lambda_1 + 8\lambda_2 + 6\lambda_4)\big) - 3(2\lambda_3 + \lambda_5)^2 - 4\beta_2^2 - 6\beta_3^2\Big]x - 128\Big[-9\lambda_1\beta_3^2 - 2(4\lambda_2 + 3\lambda_4)\beta_2^2 + 3(2\lambda_3 + \lambda_5)\beta_2\beta_3 + 3\beta_1\big(8\lambda_1(4\lambda_2 + 3\lambda_4) - (2\lambda_3 + \lambda_5)^2\big)\Big] \tag{36}$$

3.3. Electroweak minimum

By use of the three minimization equations in (9), one should therefore find a configuration from all the (σ, ϕ, Δ) space values such that the scalar potential is in a minimum situation. For such purpose, we redefine the fields in equation (5) by assuming that electroweak symmetry breaking is taking place; in this way, the structure of the potential would be energetically favored for $\langle V\rangle_{\rm EWSB} < 0$. Thereby, the naive bound on κ

$$\kappa < \kappa_{\rm max} \equiv \frac{v_\sigma^3}{2v_\phi^2 v_\Delta}\beta_1 + \frac{v_\sigma}{2v_\Delta}\beta_2 + \frac{v_\sigma v_\Delta}{2v_\phi^2}\beta_3 + \frac{v_\phi^2}{2v_\sigma v_\Delta}\lambda_1 + \frac{v_\Delta^3}{2v_\phi^2 v_\sigma}\lambda_{24}^+ + \frac{v_\Delta}{2v_\sigma}\lambda_{35}^+ \tag{37}$$

where $\lambda_{ij}^+ = \lambda_i + \lambda_j$, is a necessary and sufficient one to ensure $\langle V\rangle_{\rm EWSB} < 0$, and hence the minimum to be unique.

4. Bounds from the electroweak precision tests

To provide high precision for the 123–space parameter as an electroweak theory, additional precision has to be studied, which could impose severe bounds on the new physics. Accordingly, we highlight the Peskin-Takeuchi parameters S, T, and U [59] in the 123-model. Where the S parameter measures the deviation from the SM prediction for the electroweak (EW) radiative correction, which describes the breaking of the weak isospin symmetry, however, the T parameter measures the deviation from the SM prediction for the weak isospin symmetry breaking in the heavy sector, which is related to the difference between the masses of the W and Z bosons. In the 123-model with $v_t = 1$ or less, there is a decoupling between the doublet field and singlet field on one side and the triplet field on the other side. This decoupling is done only in the doubly charged, simply charged, and CP-odd sectors. That is to say that the major contribution of physical fields $H^\pm$, A and $H^{\pm\pm}$ comes from triplet fields, and the major contribution of physical fields h_1, h_2, h_3 and J comes from doublet and singlet fields. We use the general expressions presented in [72–75]. Approximative contributions of new scalar fields to S and T parameters in the 123-model are then given by:

$$\begin{aligned} S = \frac{1}{24\pi}\Big[&\big(U_{11}^{H\,2} + U_{12}^{H\,2} + 4U_{13}^{H\,2}\big)\ln m_{h_1}^2 + \big(U_{21}^{H\,2} + U_{22}^{H\,2} + 4U_{23}^{H\,2}\big)\ln m_{h_2}^2 \\ &+ 2\big(U_{31}^{H\,2} + U_{32}^{H\,2} + 4U_{33}^{H\,2}\big)\ln m_{h_3}^2 - \ln m_{h_{\rm ref}}^2 + \mathcal{U}_{11}^{H\,2}\hat{G}(m_{h_1}^2, m_Z^2) + \mathcal{U}_{12}^{H\,2}\hat{G}(m_{h_2}^2, m_Z^2) \\ &+ 2G(m_{h_3}^2, m_{h_3}^2, m_Z^2) - \hat{G}(m_{h_{\rm ref}}^2, m_Z^2)\Big] - \frac{1}{3\pi}\left[\ln\left(m_{H^{\pm\pm}}^2\right) - \frac{(1-2s_w^2)^2}{2}\xi\left(m_{H^{\pm\pm}}^2, m_{H^{\pm\pm}}^2, m_Z^2\right) - \frac{s_w^4}{2}\xi\left(m_{H^\pm}^2, m_{H^\pm}^2, m_Z^2\right)\right], \end{aligned} \tag{38}$$

and

$$\begin{aligned} T = \frac{1}{16\pi m_W^2 s_W^2}\Big[&F(m_{H^{\pm\pm}}^2, m_{H^\pm}^2) + U_{12}^{H\,2}F(m_{H^\pm}^2, m_{h_1}^2) + U_{22}^{H\,2}F(m_{H^\pm}^2, m_{h_2}^2) \\ &+ U_{32}^{H\,2}F(m_{H^\pm}^2, m_{h_3}^2) + 3\mathcal{U}_{11}^{H\,2}\left(F(m_Z^2, m_{h_1}^2) - F(m_W^2, m_{h_1}^2)\right) + 3\mathcal{U}_{12}^{H\,2}\left(F(m_Z^2, m_{h_2}^2)\right. \\ &\left. - F(m_W^2, m_{h_2}^2)\right) + 3\mathcal{U}_{13}^{H\,2}\left(F(m_Z^2, m_{h_3}^2) - F(m_W^2, m_{h_3}^3)\right) - 3\left(F(m_Z^2, m_{h_{\rm ref}}^2) - F(m_W^2, m_{h_{\rm ref}}^2)\right)\Big] \end{aligned} \tag{39}$$

with

$$\mathcal{U}_{11}^H = U_{11}^A U_{11}^H + U_{12}^A U_{12}^H + 2U_{13}^A U_{13}^H \tag{40}$$
$$\mathcal{U}_{12}^H = U_{11}^A U_{21}^H + U_{12}^A U_{22}^H + 2U_{13}^A U_{23}^H \tag{41}$$
$$\mathcal{U}_{13}^H = U_{11}^A U_{31}^H + U_{12}^A U_{32}^H + 2U_{13}^A U_{33}^H \tag{42}$$

whilst $m_{h_{ref}}$ stands for the SM reference represented by $m_{h_{ref}} = 125.09$ GeV, and the functions F, ξ and $\hat{G}$ can be found in Refs [72,73]. Note that, the precise measurements of the electroweak precision observables, such as the W and Z boson masses and the electroweak mixing angle, are used to determine the values of the S and T parameters. The experimental values of the S and T parameters can be used to constrain models of new physics.

Table 2
123-parameter space scan (all masses and *vev*'s are in GeV).

m_{h_1}	125
λ_2	[-6,8π]
λ_4	[-9,8π]
λ_5	[-15,14]
β_3	[-8π,8π]
κ	[0,0.1]
v_Δ	[0,1]
v_s	[10,1000]
α_1	[-π/2,π/2]
α_2	[-0.5,0.5]
α_3	[-π/2,π/2]

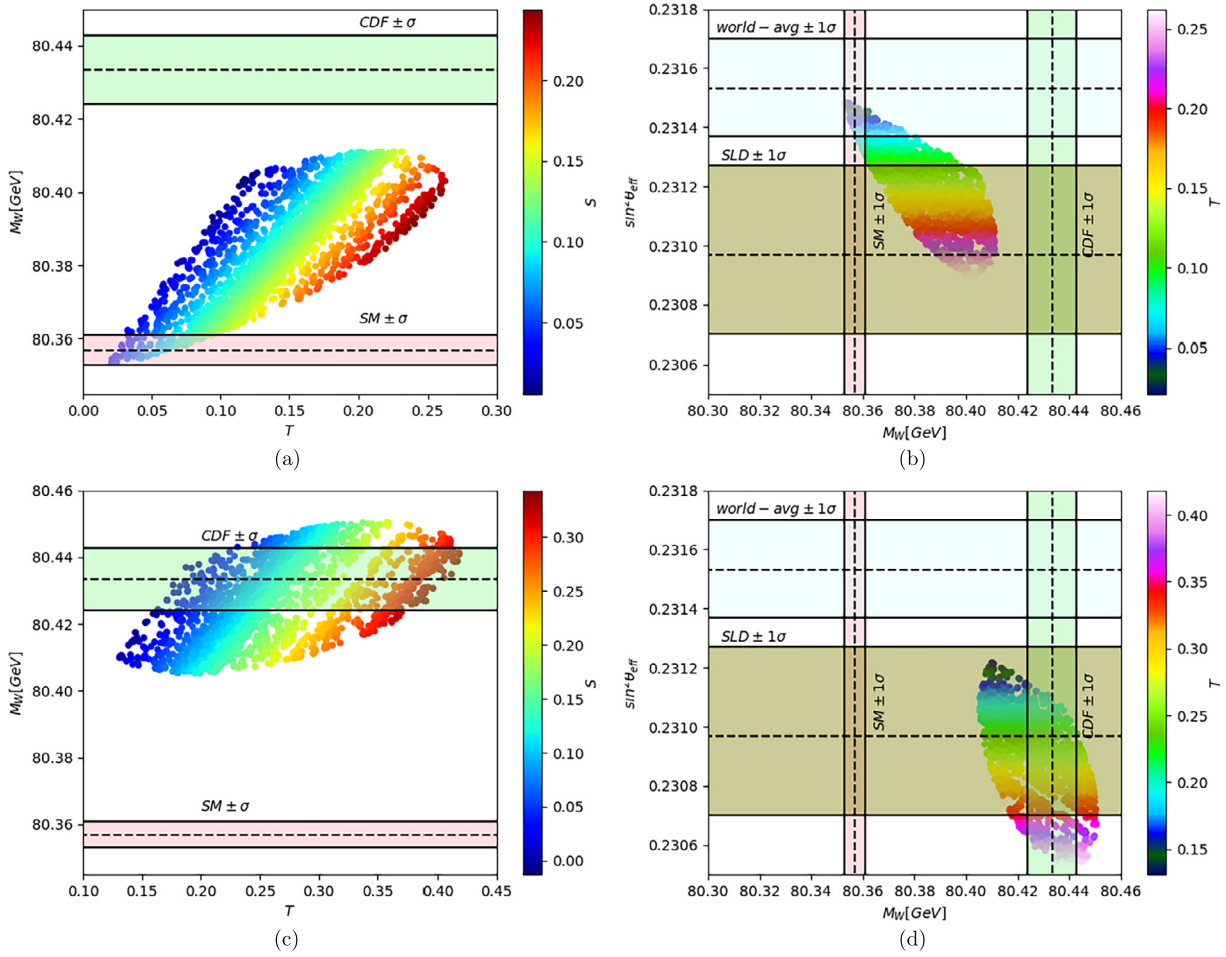

Fig. 1. Left panels: The m_W estimation in the 123-model as a function of T, where the color coding represents the size of the parameter S. The light pink bands indicate the SM prediction, while the green bands indicate the new CDF measurement for m_W, within the 1σ uncertainty. Right panels: The $\sin^2\theta_{\text{eff}}$ prediction in the 123-model as a function of m_W, with the color coding indicating the size of T. The light blue band shows the world average value for $\sin^2\theta_{\text{eff}}$ with the associated 1σ uncertainty while the brown region illustrates the result from SLD collaboration at the 1σ level. The upper (lower) panels are for the PDG (CDF) fit result.

5. Results and discussion

In order to examine whether the CDF m_W mass measurement is consistent with the 123-model's theoretical framework, we randomly scan over its parameter space as indicated in Table 2.

As previously mentioned, we assume that the CP-even h_1 plays the role of the SM-like Higgs boson with a mass near 125 GeV, which characteristics match the LHC measurements. In addition, to obtain a viable model, we require all 123-parameter points to satisfy the following theoretical and experimental constraints:

- Unitarity,[1] perturbativity, and vacuum stability requirements.

[1] We notice that such constraints were generated for the first time within this framework.

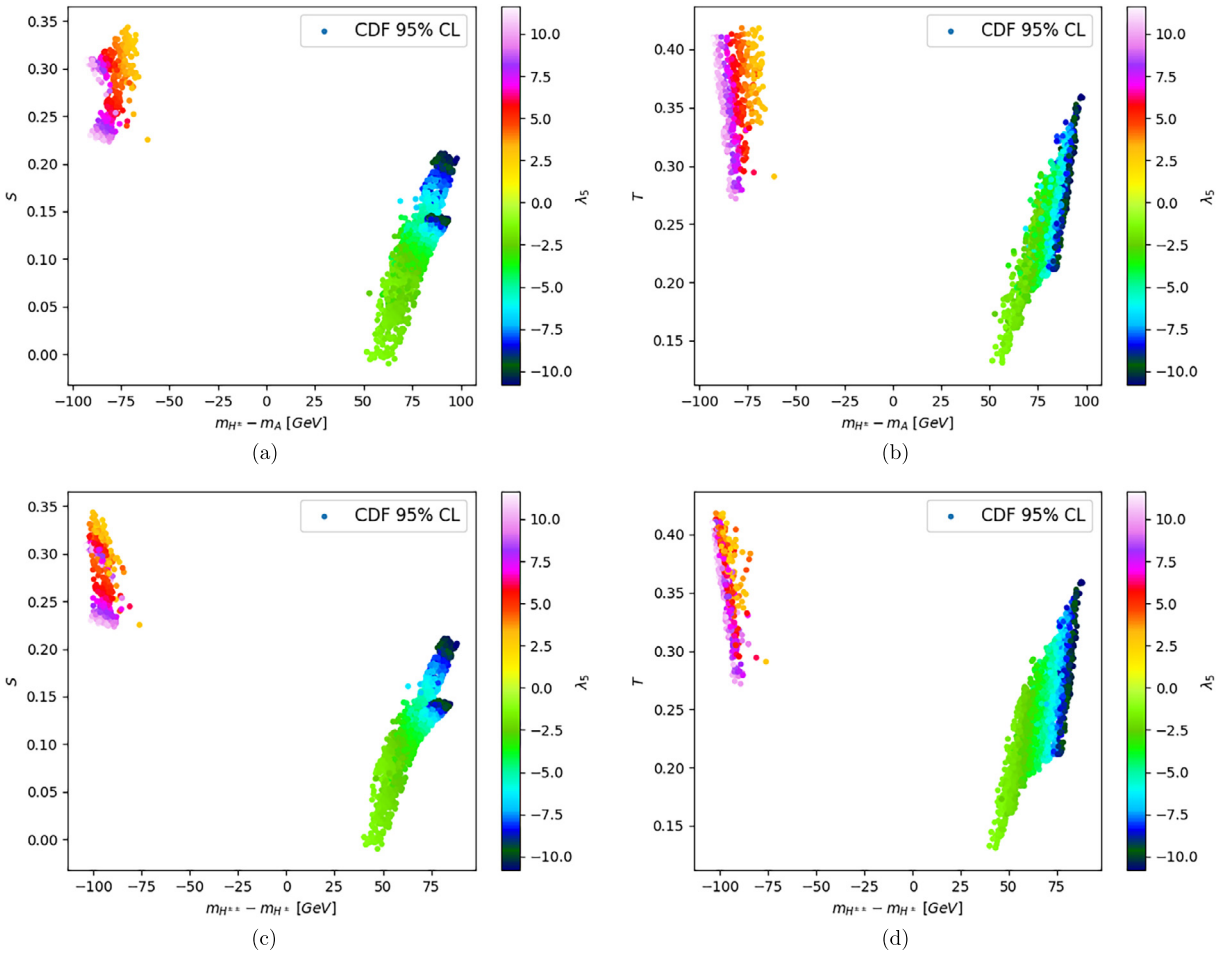

Fig. 2. Dependence of the S (left) and T (right) oblique parameters on the mass splittings $m_{H^\pm} - m_A$ and $m_{H^{\pm\pm}} - m_{H^\pm}$ with the color code indicating the λ_5 coupling. The colored regions correspond to the CDF measurement at 95%, in full consistency with theoretical and experimental constraints.

- The consistency with the 95% Bounds imposed by the LHC is checked via the public program HiggsBounds-5.10.2 [76].
- The criterion that the CP-even h_1 Higgs boson need to match the characteristics of the detected SM-like Higgs boson is enforced using the public code HiggsSignal-2.6.2 [77].
- Electro-weak precision observable (EWPO) through the oblique parameters S and T (fixing $U = 0$) using both PDG [4] and CDF [3] fit results. We applied, indeed, the test χ^2_{ST} before to and following the new $m_W^{\rm CDF}$ measurement, indicated by "PDG" and "CDF", respectively,

$$\text{PDG}: \text{S} = 0.05 \pm 0.08,\ \text{T} = 0.09 \pm 0.07,\ \rho_{\text{ST}} = 0.92 \tag{43}$$

$$\text{CDF}: \text{S} = 0.15 \pm 0.08,\ \text{T} = 0.27 \pm 0.06,\ \rho_{\text{ST}} = 0.93, \tag{44}$$

where ρ_{ST} represents the correlation between S and T.

The initial summary results are exhibited in Fig. 1 that qualitatively shows the 123-model loop contributions required by m_W measurement in view of the above PDG and CDF assessment for the oblique parameters. Firstly, by considering the PDG values, we illustrate in Fig. 1-(a) the 123-prediction for m_W as a function of T mapped over the S parameter, where the two light pink and green bands show the SM prediction and the new CDF measurement for m_W within the 1σ uncertainty. At first sight, it seems clear that the m_W value predicted by the 123-model (while passing all theoretical and experimental constraints discussed briefly above) is in line with the SM prediction, requiring $T \in [0.02, 0.10]$ and $S \in [0, 0.15]$, while are so far from the new CDF region at the 1σ level. However, the CDF bands, if χ^2_{STU}(PDG) is switched to χ^2_{STU}(CDF) in the global χ^2, can be construed within the 123-model, thereby enabling the Peskin parameters T and S to slightly lie in the ranges $0.15 - 0.42$ and $0 - 0.35$ respectively as can be seen in Fig. 1-(c).

On the other side, the right panel in Fig. 1 exhibits the model prediction for m_W with respect to $\sin^2\theta_{\rm eff}$. In such illustration, the light brown and cyan regions show respectively the SLD and world average measurement of $\sin^2\theta_{\rm eff}$ at the 1σ uncertainty. As depicted in Fig. 1-(d), after considering the CDF S, T result, the parameter points are in good compliance with only SLD measurement for $\sin^2\theta_{\rm eff}$ within the 1–1.5 σ level which is not the case when using the PDG values, where the measured value matches well both experiment predictions.

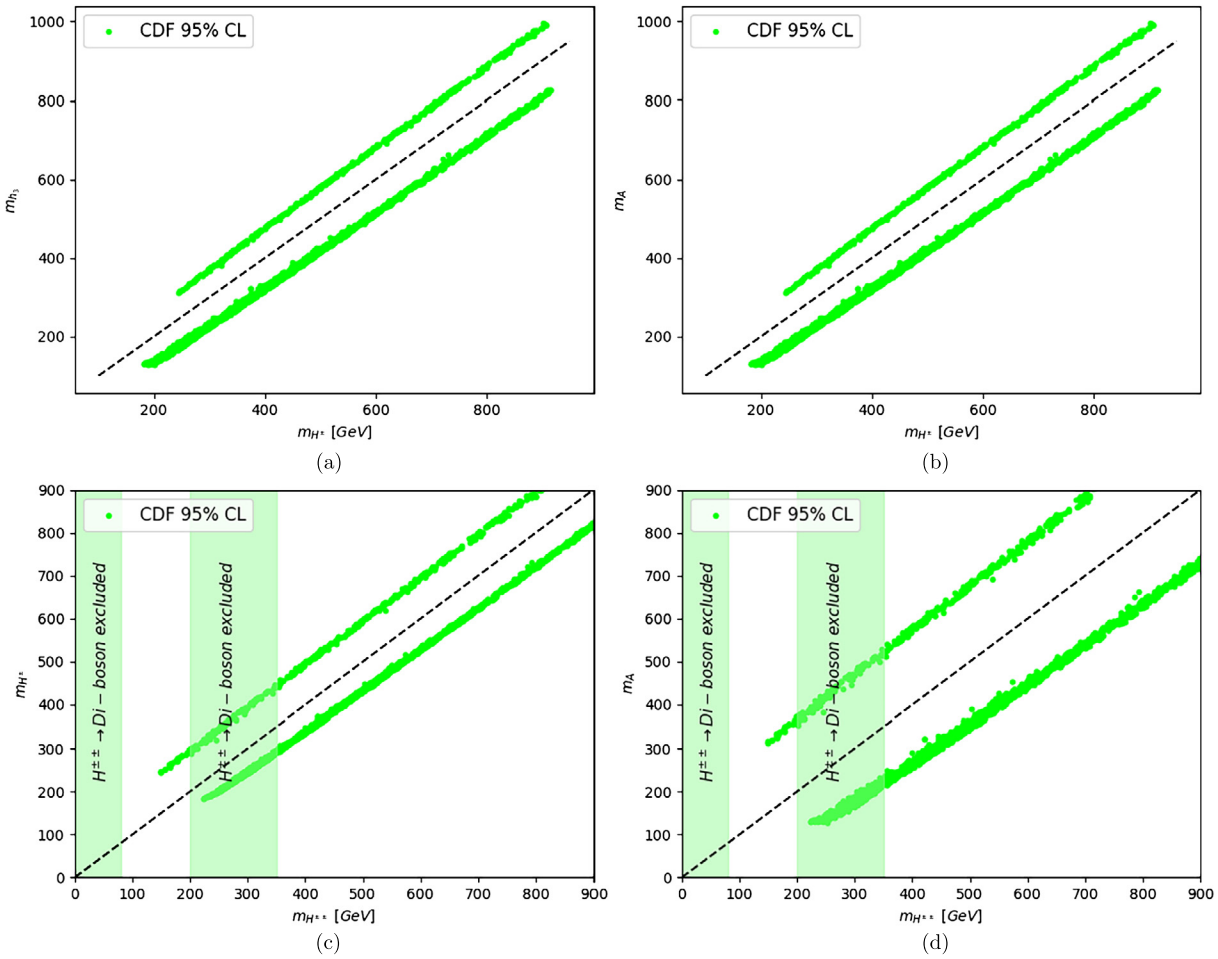

Fig. 3. Dependence of the Higgs bosons masses on each other on the light of the recent CDF (green points) measurement. The black line indicates the region of the full degenerate masses. The green bands indicate the region excluded by the $H^{\pm\pm} \to W^\pm W^\pm$.

Thereafter, we will examine how broadly the new CDF m_W, and the corresponding S and T parameters would largely affect the mass splitting between the 123-scalars, which is further illustrated in Fig. 2, where CDF S and T measurements were considered for the sake of investigation. Clearly, then, it is evident that a consistent prediction of the W boson mass in the range measured by the CDF Collaboration requires sizable mass splittings $m_{H^\pm} - m_A$ and $m_{H^{\pm\pm}} - m_{H^\pm}$ suggesting that such a m_W anomaly can be explained when there is a non-zero mass splitting among the $H^{\pm\pm}$, $H^\pm$, A. Though, in order to peer into these splittings, we have rewrite Eq. (22) into simple form as,

$$\Delta m^2 \approx m^2_{H^{\pm\pm}} - m^2_{H^\pm} \approx m^2_{H^\pm} - m^2_A \approx \frac{1}{2}(m^2_{H^{\pm\pm}} - m^2_A) \approx -\frac{\lambda_5}{4} v^2_\phi. \tag{45}$$

from which it is fairly evident that such splittings rely mainly on the λ_5 sign. Hence, for $\lambda_5 < 0$ the mass difference either between $H^\pm$ and A or $H^{\pm\pm}$ and $H^\pm$ shows the same positive sign, and predict the following hierarchy: $m_{H^\pm} - m_A > m_{H^{\pm\pm}} - m_{H^\pm}$ with a mass splitting ranging from 40 up to 90 GeV among the triplet components, while for $\lambda_5 > 0$, both splittings are negative, lying between -100 and -66 GeV. Also, it's worth mentioning that at 2σ of CDF measurement, the values of $-0.82 \lesssim \lambda_5 \lesssim 2.41$ are excluded, which therefore explains the not allowed mass splittings between roughly -75 GeV and 50 GeV.

To expand a little further on this point, we exhibit in Fig. 3 the correlation between the Higgs boson masses within two standard deviations of the CDF measurement. Off hand, one could notice how the diagonal for equal masses splits the allowed region in two, which can be expounded by the favored non-zero mass splitting as shown in Fig. 2. And more importantly, in the 123-model, as it can be seen from Fig. 3-(c) and (d), the embedded Higgs bosons are allowed to be as wide below TeV scale, whether it is for $H^\pm$, $H^{\pm\pm}$, A, and also $h_{2,3}$, which distinguishes the 123–model compared to other extensions. By way of example, these large contributions are severely constrained in HTM. Thus despite the latter is crucial, in imposing also non-zero mass splitting among new particles to express the anomaly in the W boson mass, so long as v_Δ of order GeV, the neutral heavy Higgs H and single charged Higgs H^+ masses are required to be low (450 GeV), even 350 GeV for the doubly charged scalar H^{++} [23].

Additionally, it is crucial to consider the requirements arising from collider searches. Thus, to cater to the newly measured m_W within the 123–model, we consider that $v_\Delta \preceq 1$ GeV, such that $H^{\pm\pm}$ could either contribute to Lepton Favor Violation [78], dominantly decay into same-sign lepton pairs, or two same-sign W bosons. We summarize below the experimental relevant assessments:

- For the doubly charged Higgs boson, $H^{\pm\pm}$, the latest case constitutes the main decay channel [79]

$$\Gamma(H^{\pm\pm} \to W^{\pm}W^{\pm}) = \frac{g^2 v_{\Delta}^2 m_{H^{\pm\pm}}^3}{16\pi m_W^2}\left(\frac{1}{4} - \frac{m_W^2}{m_{H^{\pm\pm}}^2} + \frac{3m_W^4}{m_{H^{\pm\pm}}^4}\right)\sqrt{1 - 4\frac{m_W^2}{m_{H^{\pm\pm}}^2}} \tag{46}$$

  and a lower bound has been revised [80,81] to be $m_{H^{\pm\pm}} \geq 84$ GeV, while studying $H^{\pm\pm}$ in the $4W$ final state rules out the $m_{H^{\pm\pm}}$ (in GeV) from 200 up to 350 [82], as signaled in Fig. 2-(c) and (d). However, in the remaining mass window between 84 and 200 (in GeV), the $H^{\pm\pm}$ is the lightest compared to all the 123–model Higgs bosons; i.e., $m_{A/h_{2,3}} \geq m_{H^{\pm}} \geq m_{H^{\pm\pm}}$, so that the $l^{\pm}l^{\pm}$ di-lepton decay could have gotten close to the same sign di-boson one, $W^{\pm *}W^{\pm *}$.
- For the remaining Higgs bosons, it is also very important to note that situation of degenerate $H^{\pm}$ with either h_2 or h_3 is slightly unfavorite by the CDF measurement. More so, only the case were $m_{H^{\pm}} - m_{h2} > 0$ and $m_{H^{\pm}} - m_{h3} < 0$ is allowed. It is noteworthy that CDF measurement has also imposed stringent restrictions on CP odd Higgs boson m_A, thus avoiding a possible degeneration of mass with the simply charged Higgs boson $H^{\pm}$, by preferring a positive splitting: $m_{H^{\pm}} - m_A > 0$.

6. Conclusion

The CDF II experiment has reported a significant anomaly for the W boson mass. And, with remarkable precision, it reveals a slightly higher value compared to the SM value. This intriguing deviation continues to be actively investigated, as it could potentially signify the presence of new physics BSM. It is also plausible that such discrepancy stems from systematic uncertainties or other contributing factors rather than new physics. Further in-depth studies are necessary to fully comprehend the origin of this deviation and its implications in the realm of particle physics.

In this paper, we have discussed the consistency of the aforementioned anomaly within the 123-model, while considering the theoretical and experimental constraints. Accordingly, as the provided Higgs spectrum is phenomenologically diverse, the impacts of the fields involved VEVs v_{σ} and v_{Δ} at the tree level could affect on S and T oblique parameters, and thus can dramatically change the W-boson mass from what the SM predicts. We found that, the new m_W measured at CDF-II experiments favorite non-zero mass splitting among the h_2, h_3, A, $H^{\pm}$ and $H^{\pm\pm}$.

All the above, it is noteworthy that the precise measurements of the W boson mass made by CDF, and many other experiments, continue to play a crucial part in putting the SM to the test and in the quest for novel physics outside of the SM.

Declaration of competing interest

The authors declare that they have no known competing financial interests or personal relationships that could have appeared to influence the work reported in this paper.

Data availability

No data was used for the research described in the article.

References

[1] ATLAS Collaboration, G. Aad, et al., Observation of a new particle in the search for the Standard Model Higgs boson with the ATLAS detector at the LHC, Phys. Lett. B 716 (2012) 1–29, arXiv:1207.7214.
[2] CMS Collaboration, S. Chatrchyan, et al., Observation of a new boson at a mass of 125 GeV with the CMS experiment at the LHC, Phys. Lett. B 716 (2012) 30–61, arXiv:1207.7235.
[3] CDF Collaboration, T. Aaltonen, et al., High-precision measurement of the W boson mass with the CDF II detector, Science 376 (6589) (2022) 170–176.
[4] Particle Data Group Collaboration, P.A. Zyla, et al., Rev. Part. Phys., PTEP 2020 (8) (2020), 083C01.
[5] M. Awramik, M. Czakon, A. Freitas, G. Weiglein, Precise prediction for the W boson mass in the standard model, Phys. Rev. D 69 (2004) 053006, arXiv:hep-ph/0311148.
[6] C.-T. Lu, L. Wu, Y. Wu, B. Zhu, Electroweak precision fit and new physics in light of W boson mass, arXiv:2204.03796.
[7] Y.-Z. Fan, T.-P. Tang, Y.-L.S. Tsai, L. Wu, Inert Higgs dark matter for new CDF W-boson mass and detection prospects, arXiv:2204.03693.
[8] C.-R. Zhu, M.-Y. Cui, Z.-Q. Xia, Z.-H. Yu, X. Huang, Q. Yuan, Y.Z. Fan, GeV antiproton/gamma-ray excesses and the W-boson mass anomaly: three faces of $\sim 60-70$ GeV dark matter particle?, arXiv:2204.03767.
[9] B.-Y. Zhu, S. Li, J.-G. Cheng, R.-L. Li, Y.-F. Liang, Using gamma-ray observation of dwarf spheroidal galaxy to test a dark matter model that can interpret the W-boson mass anomaly, arXiv:2204.04688.
[10] H. Song, W. Su, M. Zhang, Electroweak phase transition in 2HDM under Higgs, Z-pole, and W precision measurements, arXiv:2204.05085.
[11] H. Bahl, J. Braathen, G. Weiglein, New physics effects on the W-boson mass from a doublet extension of the SM Higgs sector, arXiv:2204.05269.
[12] Y. Heo, D.-W. Jung, J.S. Lee, Impact of the CDF W-mass anomaly on two Higgs doublet model, arXiv:2204.05728.
[13] K.S. Babu, S. Jana, P.K. Vishnu, Correlating W-boson mass shift with muon $g-2$ in the 2HDM, arXiv:2204.05303.
[14] T. Biekötter, S. Heinemeyer, G. Weiglein, Excesses in the low-mass Higgs-boson search and the W-boson mass measurement, arXiv:2204.05975.
[15] Y.H. Ahn, S.K. Kang, R. Ramos, Implications of new CDF-II W boson mass on two Higgs doublet model, arXiv:2204.06485.
[16] X.-F. Han, F. Wang, L. Wang, J.M. Yang, Y. Zhang, A joint explanation of W-mass and muon g-2 in 2HDM, arXiv:2204.06505.
[17] G. Arcadi, A. Djouadi, The 2HD+a model for a combined explanation of the possible excesses in the CDF $\mathbf{M_W}$ measurement and $(\mathbf{g-2})_{\mu}$ with dark matter, arXiv:2204.08406.
[18] K. Ghorbani, P. Ghorbani, W-boson mass anomaly from scale invariant 2HDM, arXiv:2204.09001.
[19] H. Abouabid, A. Arhrib, R. Benbrik, M. Krab, M. Ouchemhou, Is the new CDF M_W measurement consistent with the two Higgs doublet model?, arXiv:2204.12018.
[20] R. Benbrik, M. Boukidi, B. Manaut, W-mass and 96 GeV excess in type-III 2HDM, arXiv:2204.11755.
[21] Y. Cheng, X.-G. He, Z.-L. Huang, M.-W. Li, Type-II seesaw triplet scalar and its VEV effects on neutrino trident scattering and W mass, arXiv:2204.05031.
[22] X.K. Du, Z. Li, F. Wang, Y.K. Zhang, Explaining the new CDF II W-boson mass data in the Georgi-Machacek extension models, arXiv:2204.05760.
[23] S. Kanemura, K. Yagyu, Implication of the W boson mass anomaly at CDF II in the Higgs triplet model with a mass difference, arXiv:2204.07511.
[24] P. Mondal, Enhancement of the **W** boson mass in the Georgi-Machacek model, arXiv:2204.07844.
[25] D. Borah, S. Mahapatra, D. Nanda, N. Sahu, Type II Dirac seesaw with observable ΔN_{eff} in the light of W-mass anomaly, arXiv:2204.08266.
[26] J.M. Yang, Y. Zhang, Low energy SUSY confronted with new measurements of W-boson mass and muon g-2, arXiv:2204.04202.

[27] X.K. Du, Z. Li, F. Wang, Y.K. Zhang, Explaining the muon $g-2$ anomaly and new CDF II W-boson mass in the framework of (extra)ordinary gauge mediation, arXiv:2204.04286.
[28] P. Athron, M. Bach, D.H.J. Jacob, W. Kotlarski, D. Stöckinger, A. Voigt, Precise calculation of the W boson pole mass beyond the Standard Model with FlexibleSUSY, arXiv:2204.05285.
[29] M.-D. Zheng, F.-Z. Chen, H.-H. Zhang, The $W\ell\nu$-vertex corrections to W-boson mass in the R-parity violating MSSM, arXiv:2204.06541.
[30] A. Ghoshal, N. Okada, S. Okada, D. Raut, Q. Shafi, A. Thapa, Type III seesaw with R-parity violation in light of m_W (CDF), arXiv:2204.07138.
[31] P. Athron, A. Fowlie, C.-T. Lu, L. Wu, Y. Wu, B. Zhu, The W boson mass and muon $g-2$: hadronic uncertainties or new physics?, arXiv:2204.03996.
[32] K. Cheung, W.-Y. Keung, P.-Y. Tseng, Iso-doublet vector leptoquark solution to the muon $g-2$, R_{K,K^*}, R_{D,D^*}, and W-mass anomalies, arXiv:2204.05942.
[33] A. Bhaskar, A.A. Madathil, T. Mandal, S. Mitra, Combined explanation of W-mass, muon $g-2$, $R_{K^{(*)}}$ and $R_{D^{(*)}}$ anomalies in a singlet-triplet scalar leptoquark model, arXiv:2204.09031.
[34] M. Blennow, P. Coloma, E. Fernández-Martínez, M. González-López, Right-handed neutrinos and the CDF II anomaly, arXiv:2204.04559.
[35] F. Arias-Aragón, E. Fernández-Martínez, M. González-López, L. Merlo, Dynamical minimal flavour violating inverse seesaw, arXiv:2204.04672.
[36] X. Liu, S.-Y. Guo, B. Zhu, Y. Li, Unifying gravitational waves with W boson, FIMP dark matter, and Majorana Seesaw mechanism, arXiv:2204.04834.
[37] T.A. Chowdhury, J. Heeck, S. Saad, A. Thapa, W boson mass shift and muon magnetic moment in the Zee model, arXiv:2204.08390.
[38] O. Popov, R. Srivastava, The triplet Dirac seesaw in the view of the recent CDF-II W mass anomaly, arXiv:2204.08568.
[39] H.M. Lee, K. Yamashita, A model of vector-like leptons for the muon $g-2$ and the W boson mass, arXiv:2204.05024.
[40] J. Kawamura, S. Okawa, Y. Omura, W boson mass and muon $g-2$ in a lepton portal dark matter model, arXiv:2204.07022.
[41] A. Crivellin, M. Kirk, T. Kitahara, F. Mescia, Correlating $t\to cZ$ to the W mass and B physics with vector-like quarks, arXiv:2204.05962.
[42] K.I. Nagao, T. Nomura, H. Okada, A model explaining the new CDF II W boson mass linking to muon $g-2$ and dark matter, arXiv:2204.07411.
[43] T.A. Chowdhury, S. Saad, Leptoquark-vectorlike quark model for the CDF mW, (g-2)μ, RK(*) anomalies, and neutrino masses, Phys. Rev. D 106 (5) (2022) 055017, arXiv:2205.03917.
[44] J. Cao, L. Meng, L. Shang, S. Wang, B. Yang, Interpreting the W-mass anomaly in vectorlike quark models, Phys. Rev. D 106 (5) (2022) 055042, arXiv:2204.09477.
[45] A. Strumia, Interpreting electroweak precision data including the W-mass CDF anomaly, arXiv:2204.04191.
[46] L.M. Carpenter, T. Murphy, M.J. Smylie, Changing patterns in electroweak precision with new color-charged states: oblique corrections and the W boson mass, arXiv:2204.08546.
[47] M. Du, Z. Liu, P. Nath, CDF W mass anomaly from a dark sector with a Stueckelberg-Higgs portal, arXiv:2204.09024.
[48] G.-W. Yuan, L. Zu, L. Feng, Y.-F. Cai, Y.-Z. Fan, Hint on new physics from the W-boson mass excess—axion-like particle, dark photon or chameleon dark energy, arXiv:2204.04183.
[49] G. Cacciapaglia, F. Sannino, The W boson mass weighs in on the non-standard Higgs, arXiv:2204.04514.
[50] K. Sakurai, F. Takahashi, W. Yin, Singlet extensions and W boson mass in the light of the CDF II result, arXiv:2204.04770.
[51] J.J. Heckman, Extra W-boson mass from a D3-brane, arXiv:2204.05302.
[52] N.V. Krasnikov, Nonlocal generalization of the SM as an explanation of recent CDF result, arXiv:2204.06327.
[53] Z. Péli, Z. Trócsányi, Vacuum stability and scalar masses in the superweak extension of the standard model, arXiv:2204.07100.
[54] P. Fileviez Perez, H.H. Patel, A.D. Plascencia, On the W-mass and new Higgs bosons, arXiv:2204.07144.
[55] R.A. Wilson, A toy model for the W/Z mass ratio, arXiv:2204.07970.
[56] K.-Y. Zhang, W.-Z. Feng, Explaining W boson mass anomaly and dark matter with a $U(1)$ dark sector, arXiv:2204.08067.
[57] M. Algueró, J. Matias, A. Crivellin, C.A. Manzari, Unified explanation of the anomalies in semileptonic B decays and the W mass, Phys. Rev. D 106 (3) (2022) 033005, arXiv:2201.08170.
[58] W. Abdallah, R. Gandhi, S. Roy, LSND and MiniBooNE as guideposts to understanding the muon (g-2) results and the CDF II W mass measurement, Phys. Lett. B 840 (2023) 137841, arXiv:2208.02264.
[59] M.E. Peskin, T. Takeuchi, Estimation of oblique electroweak corrections, Phys. Rev. D 46 (1992) 381–409.
[60] J. Schechter, J.W.F. Valle, Neutrino decay and spontaneous violation of lepton number, Phys. Rev. D 25 (1982) 774.
[61] M.A. Diaz, M.A. Garcia-Jareno, D.A. Restrepo, J.W.F. Valle, Seesaw majoron model of neutrino mass and novel signals in Higgs boson production at LEP, Nucl. Phys. B 527 (1998) 44–60, arXiv:hep-ph/9803362.
[62] A.G. Akeroyd, M.A. Diaz, M.A. Rivera, D. Romero, Fermiophobia in a Higgs triplet model, Phys. Rev. D 83 (2011) 095003, arXiv:1010.1160.
[63] S. Blunier, G. Cottin, M.A. Díaz, B. Koch, Phenomenology of a Higgs triplet model at future e^+e^- colliders, Phys. Rev. D 95 (7) (2017) 075038, arXiv:1611.07896.
[64] Particle Data Group Collaboration, C. Patrignani, et al., Rev. Part. Phys., Chin. Phys. C 40 (10) (2016) 100001.
[65] Particle Data Group Collaboration, K.A. Olive, et al., Rev. Part. Phys., Chin. Phys. C 38 (2014) 090001.
[66] M. Carena, A. de Gouvea, A. Freitas, M. Schmitt, Invisible Z boson decays at e+ e- colliders, Phys. Rev. D 68 (2003) 113007, arXiv:hep-ph/0308053.
[67] A. Arhrib, R. Benbrik, M. Chabab, G. Moultaka, M.C. Peyranere, L. Rahili, J. Ramadan, The Higgs potential in the type II seesaw model, Phys. Rev. D 84 (2011) 095005, arXiv:1105.1925.
[68] C. Bonilla, R.M. Fonseca, J.W.F. Valle, Consistency of the triplet seesaw model revisited, Phys. Rev. D 92 (7) (2015) 075028, arXiv:1508.02323.
[69] B.A. Ouazghour, A. Arhrib, R. Benbrik, M. Chabab, L. Rahili, Theory and phenomenology of a two-Higgs-doublet type-II seesaw model at the LHC run 2, Phys. Rev. D 100 (3) (2019) 035031, arXiv:1812.07719.
[70] A. Arhrib, R. Benbrik, M. El Kacimi, L. Rahili, S. Semlali, Extended Higgs sector of 2HDM with real singlet facing LHC data, Eur. Phys. J. C 80 (1) (2020) 13, arXiv:1811.12431.
[71] J.a.P. Pinheiro, C.A. de, S. Pires, Vacuum stability and spontaneous violation of the lepton number at a low-energy scale in a model for light sterile neutrinos, Phys. Rev. D 102 (1) (2020) 015015, arXiv:2003.02350.
[72] S. Ghosh, Oblique parameters of BSM models with three CP-even neutral scalars, arXiv:2201.01006.
[73] L. Lavoura, L.-F. Li, Making the small oblique parameters large, Phys. Rev. D 49 (1994) 1409–1416, arXiv:hep-ph/9309262.
[74] W. Grimus, L. Lavoura, O. Ogreid, P. Osland, A precision constraint on multi-Higgs-doublet models, J. Phys. G, Nucl. Part. Phys. 35 (7) (2008) 075001.
[75] W. Grimus, L. Lavoura, O. Ogreid, P. Osland, The oblique parameters in multi-Higgs-doublet models, Nucl. Phys. B 801 (1–2) (2008) 81–96.
[76] P. Bechtle, D. Dercks, S. Heinemeyer, T. Klingl, T. Stefaniak, G. Weiglein, J. Wittbrodt, HiggsBounds-5: testing Higgs sectors in the LHC 13 TeV era, Eur. Phys. J. C 80 (12) (2020) 1211, arXiv:2006.06007.
[77] P. Bechtle, S. Heinemeyer, T. Klingl, T. Stefaniak, G. Weiglein, J. Wittbrodt, HiggsSignals-2: probing new physics with precision Higgs measurements in the LHC 13 TeV era, Eur. Phys. J. C 81 (2) (2021) 145, arXiv:2012.09197.
[78] J. Gluza, M. Kordiaczynska, T. Srivastava, Discriminating the HTM and MLRSM models in collider studies via doubly charged Higgs boson pair production and the subsequent leptonic decays, Chin. Phys. C 45 (7) (2021) 073113, arXiv:2006.04610.
[79] Z. Kang, J. Li, T. Li, Y. Liu, G.-Z. Ning, Light doubly charged Higgs boson via the WW^* channel at LHC, Eur. Phys. J. C 75 (12) (2015) 574, arXiv:1404.5207.
[80] ATLAS Collaboration, G. Aad, et al., Search for anomalous production of prompt same-sign lepton pairs and pair-produced doubly charged Higgs bosons with $\sqrt{s}=8$ TeV pp collisions using the ATLAS detector, J. High Energy Phys. 03 (2015) 041, arXiv:1412.0237.
[81] S. Kanemura, M. Kikuchi, H. Yokoya, K. Yagyu, LHC run-I constraint on the mass of doubly charged Higgs bosons in the same-sign diboson decay scenario, PTEP 2015 (2015) 051B02, arXiv:1412.7603.
[82] ATLAS Collaboration, G. Aad, et al., Search for doubly and singly charged Higgs bosons decaying into vector bosons in multi-lepton final states with the ATLAS detector using proton-proton collisions at $\sqrt{s}=13$ TeV, J. High Energy Phys. 06 (2021) 146, arXiv:2101.11961.